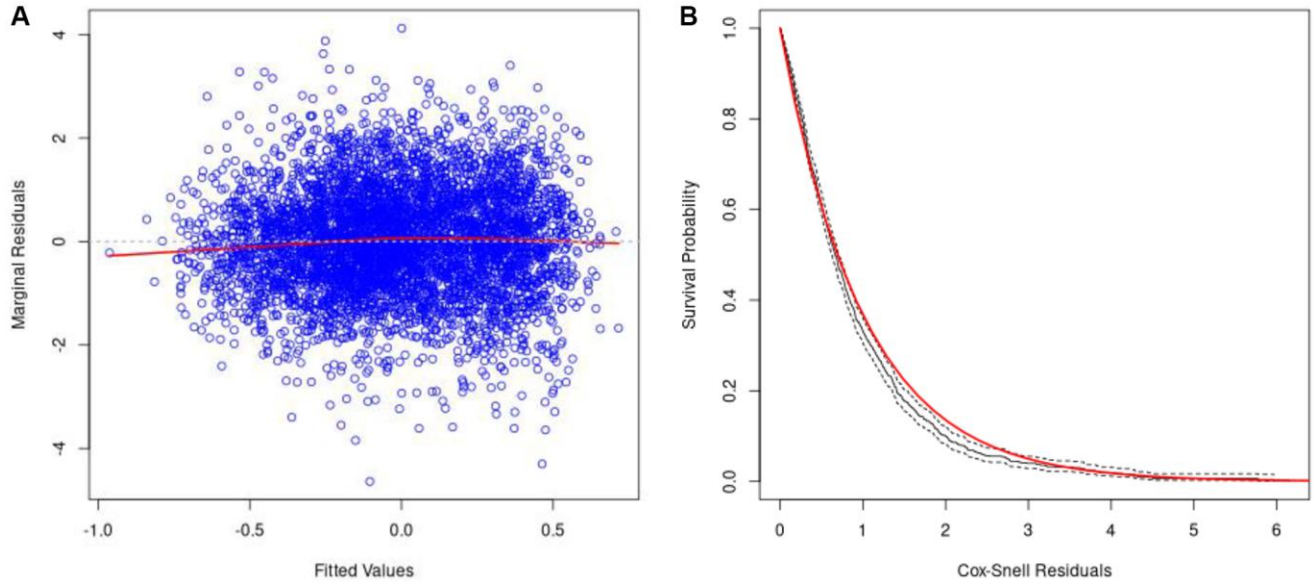
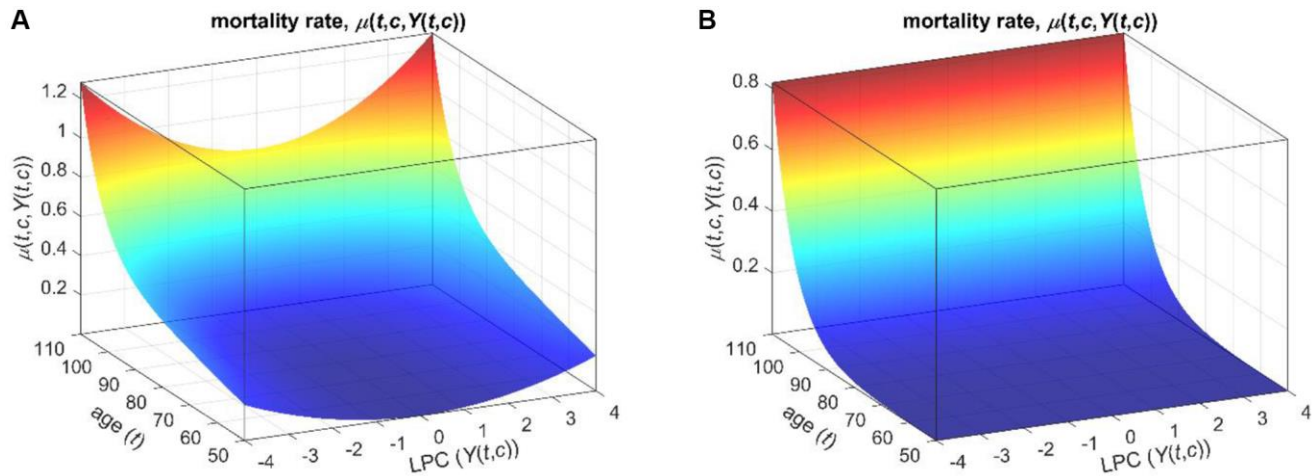


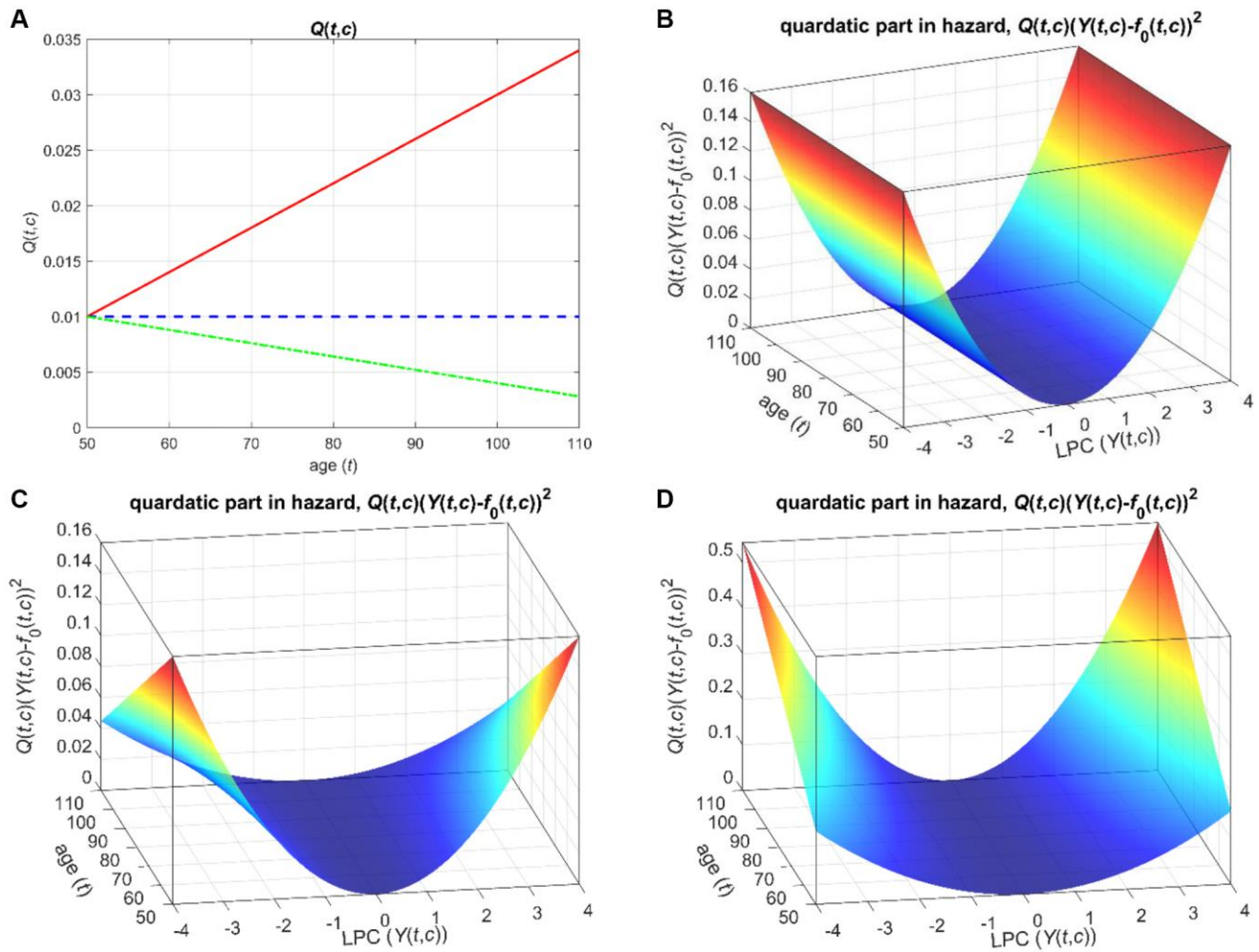
SUPPLEMENTARY FIGURES



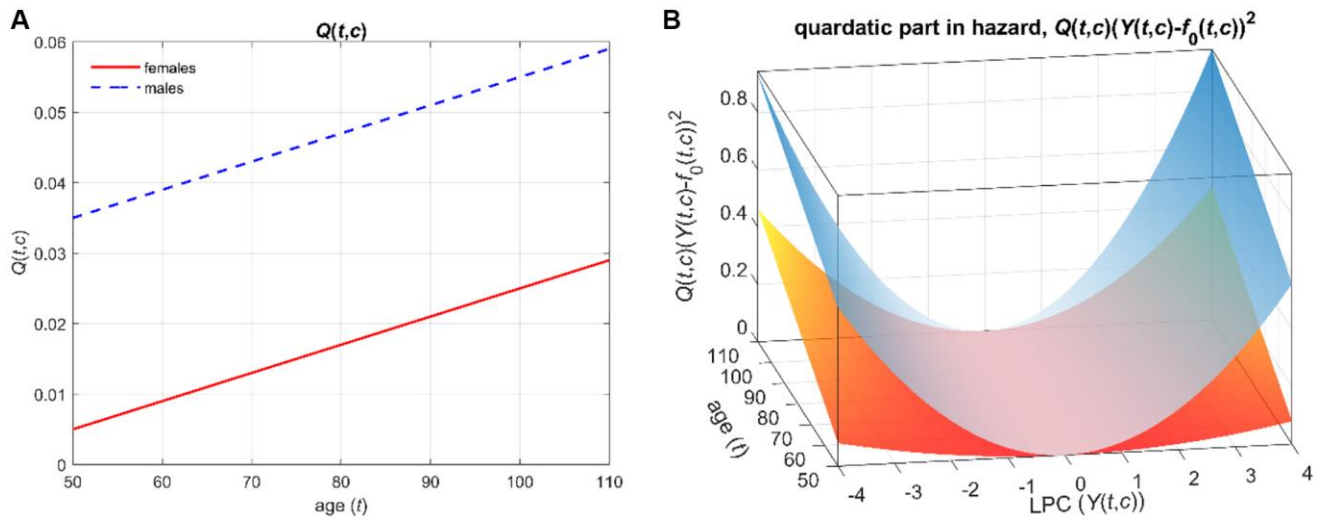
Supplementary Figure 1. Diagnostic plots assessing the goodness-of-fit and assumptions of joint models in applications to LPC 15:0/0:0. (A) Plot of the standardized marginal residuals versus the corresponding fitted values for the longitudinal outcome (LPC 15:0/0:0). The red solid line denotes the fit of the loess smoother. (B) Residuals analysis for the survival outcome by assessing the overall fit of the survival sub-model using the Cox-Snell residuals. The black solid line denotes the Kaplan-Meier estimate of the survival function of the residuals (with the dashed lines corresponding to the 95% pointwise confidence intervals). The red solid line is the survival function of the unit exponential distribution (this is the distribution if the survival sub-model is correct).



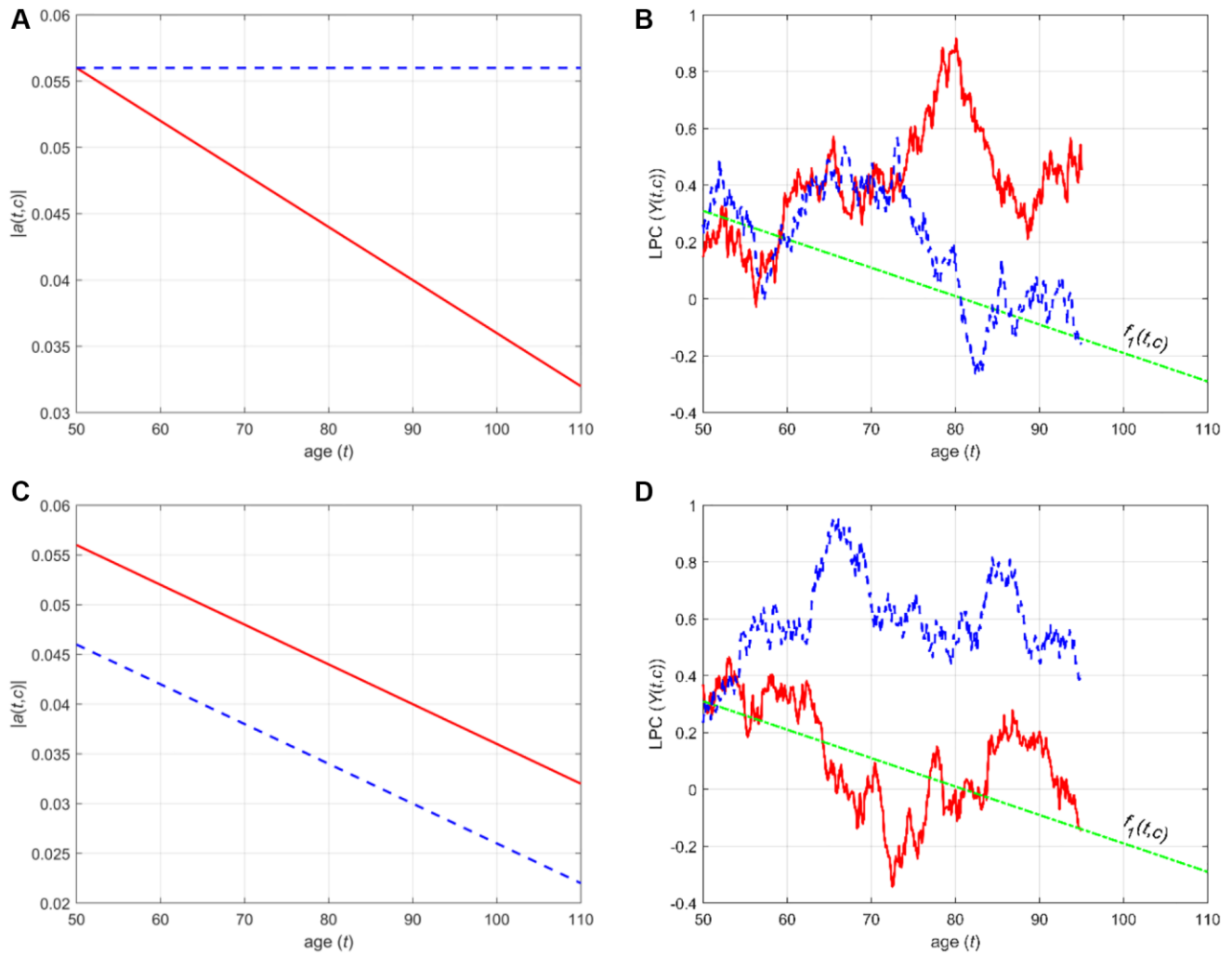
Supplementary Figure 2. Stochastic process models: 3D plots illustrating mortality rates corresponding to different quadratic hazard terms $Q(t, c)$. (A) Mortality rate in the case of non-zero $Q(t, c)$; (B) Mortality rate when $Q(t, c) = 0$. For this illustration, we modeled Eqs. (6–7) with a single binary covariate c and parameters corresponding to a hypothetical biomarker $Y(t, c)$ (e.g., a transformed LPC) having the standard normal distribution and hazard rates resembling human mortality rates at old ages. The figures display the mortality rate $\mu(t, c, Y(t, c))$ (Eq. (7)) as a function of age t , covariate c (shown for $c = 0$), and the hypothetical biomarker $Y(t, c)$.



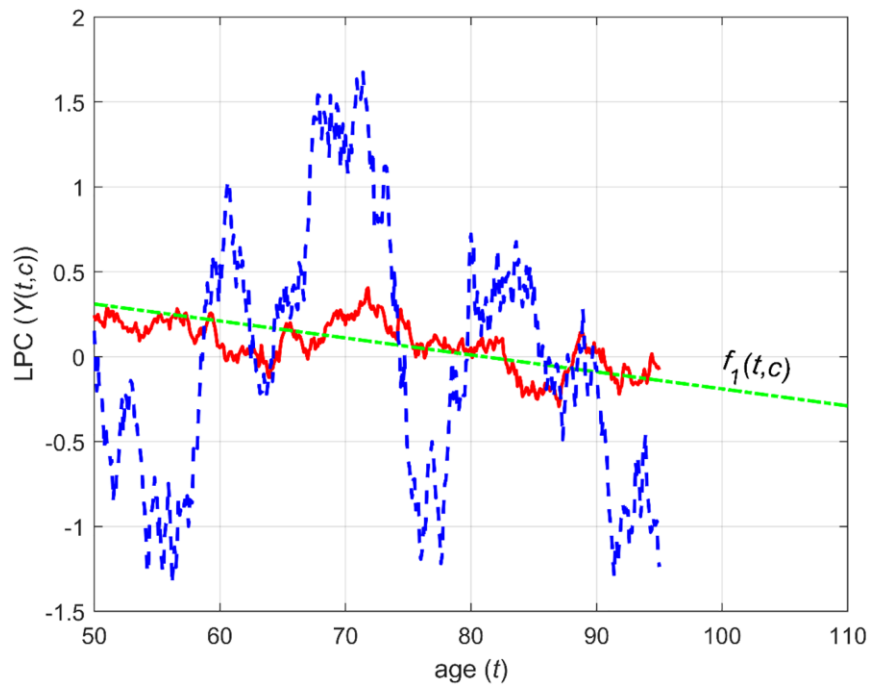
Supplementary Figure 3. Stochastic process models: Illustration of the quadratic part in the hazard corresponding to different age patterns of $Q(t, c)$. (A) Age patterns of $Q(t, c)$: age-independent (dashed blue line), declining with age (dash-dotted green line), and increasing with age (solid red line); (B) The quadratic part in the hazard in the case of age-independent $Q(t, c)$; (C) The quadratic part in the hazard corresponding to $Q(t, c)$ declining with age; (D) The quadratic part in the hazard when $Q(t, c)$ is increasing with age. For this illustration, we modeled Eqs. (6–7) with a single binary covariate c and parameters corresponding to a hypothetical biomarker $Y(t, c)$ (e.g., a transformed LPC) having the standard normal distribution and hazard rates resembling human mortality rates at old ages. The figures (B–D) display the quadratic part in the hazard in Eq. (7) (i.e., $Q(t, c)(Y(t, c) - f_0(t, c))^2$) as a function of age t , covariate c (shown for $c = 0$), and the hypothetical biomarker $Y(t, c)$ for respective $Q(t, c)$ modeled as a linear function of age t and covariate c . We assumed $f_0(t, c) = 0$ for simplicity of illustration.



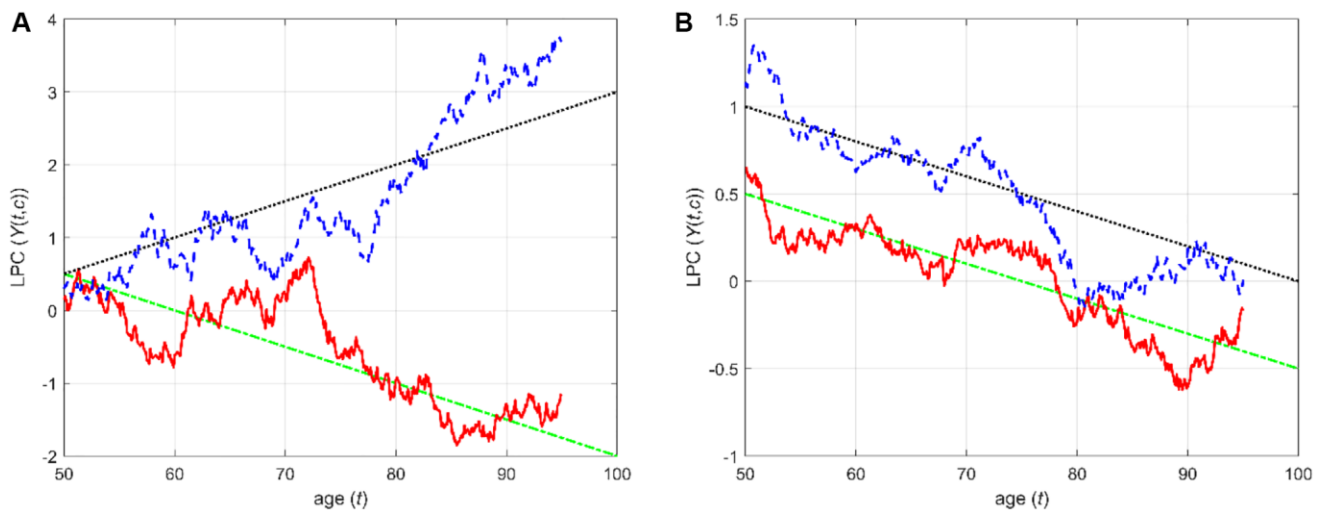
Supplementary Figure 4. Stochastic process models: Illustration of the quadratic part in the hazard corresponding to different patterns of $Q(t, c)$ in females and males. (A) Age patterns of $Q(t, c)$ in females (solid red line) and males (dashed blue line); b) The quadratic part in the hazard corresponding to female (surface at the bottom) and male (surface at the top) $Q(t, c)$. For this illustration, we modeled Eqs. (6–7) with a single binary covariate c (sex) and parameters corresponding to a hypothetical biomarker $Y(t, c)$ (e.g., a transformed LPC) having the standard normal distribution and hazard rates resembling human mortality rates at old ages. The surfaces in (B) show the quadratic part in the hazard in Eq. (7) (i.e., $Q(t, c)(Y(t, c) - f_0(t, c))^2$) as a function of age t , covariate c ($c = 0$ for females, $c = 1$ for males), and the hypothetical biomarker $Y(t, c)$ for respective $Q(t, c)$ modeled as a linear function of age t and covariate c as shown in Figure A). We assumed $f_0(t, c) = \mathbf{0}$ for simplicity of illustration.



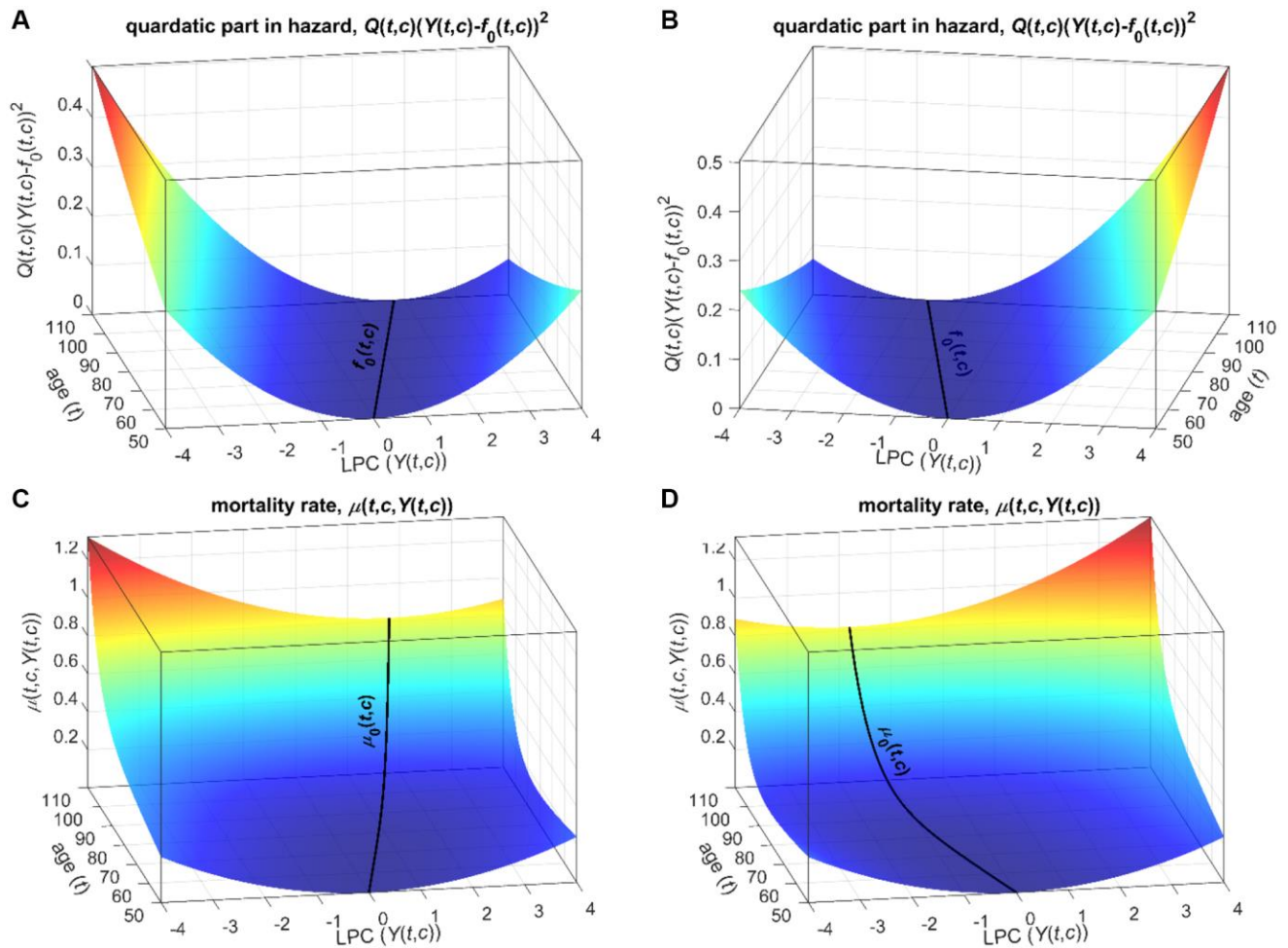
Supplementary Figure 5. Stochastic process models: Illustration of the patterns of the feedback coefficient and sample age trajectories of the process $Y(t, c)$. (A) Age-independent (dashed blue line) and declining (solid red line) patterns of the absolute value of the feedback coefficient ($|a(t, c)|$); (B) Sample trajectories of $Y(t, c)$ corresponding to respective patterns of $|a(t, c)|$ shown in (A); (C) Age patterns of $|a(t, c)|$ for females (solid red line) and males (dashed blue line); (D) Sample trajectories of $Y(t, c)$ in females (solid red line) and males (dashed blue line) corresponding to respective patterns of $|a(t, c)|$ shown in (C). For this illustration, we modeled Eq. (6) for a hypothetical biomarker $Y(t, c)$ (e.g., a transformed LPC) with respective patterns of the feedback coefficient $a(t, c)$ and a single binary covariate c (sex). The sample trajectories of $Y(t, c)$ shown in (B) and (D) were generated from respective distributions with feedback coefficients shown in (A) and (C). We assumed that the equilibrium levels $f_1(t, c)$ (shown as dash-dotted green lines in (B) and (D)) are similar in both cases, for simplicity of illustration.



Supplementary Figure 6. Stochastic process models: Examples of trajectories of the stochastic process $Y(t, c)$ with different volatility coefficients. The figure shows sample trajectories of $Y(t, c)$ in the stochastic process models corresponding to higher (dashed blue line) and lower (solid red line) volatility coefficients $b(t, c)$. For this illustration, we modeled Eq. (6) for a hypothetical biomarker $Y(t, c)$ (e.g., a transformed LPC). The sample trajectories of $Y(t, c)$ were generated from respective distributions with different values of the volatility coefficients $b(t, c)$ ($b(t, c) = 0.1$ and $b(t, c) = 0.4$). We assumed that the equilibrium levels $f_1(t, c)$ (shown as the dash-dotted green line) are similar in both cases, for simplicity of illustration.

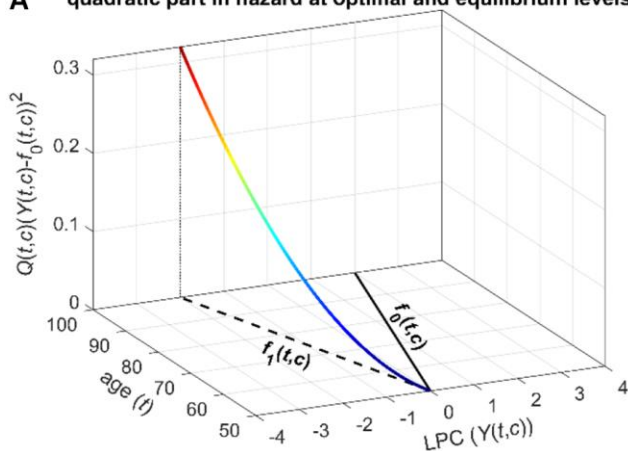


Supplementary Figure 7. Stochastic process models: Examples of trajectories of the stochastic process $Y(t, c)$ with different equilibrium patterns. (A) This figure shows two equilibrium trajectories with increasing (black dotted line) and decreasing (green dash-dotted line) age patterns and corresponding sample trajectories of $Y(t, c)$ (blue dashed and red solid lines, respectively); (B) This figure shows two equilibrium trajectories shifted by a constant (e.g., representing sex-specific equilibrium levels in the model) (black dotted and green dash-dotted lines) and corresponding sample trajectories of $Y(t, c)$ (blue dashed and red solid lines, respectively). For this illustration, we modeled Eq. (6) for a hypothetical biomarker $Y(t, c)$ (e.g., a transformed LPC) with $f_1(t, c) = a_{f_1} + b_{f_1}(t - t_{\min}) + \beta_{f_1}c$ and a single binary covariate c (sex). The sample trajectories of $Y(t, c)$ were generated from respective distributions with different parameters in $f_1(t, c)$ (positive and negative b_{f_1} and zero β_{f_1} in (A), negative b_{f_1} and positive β_{f_1} in (B)) so that the black dotted and blue dashed lines correspond to the equilibrium levels and a sample trajectory of $Y(t, c)$ for males).

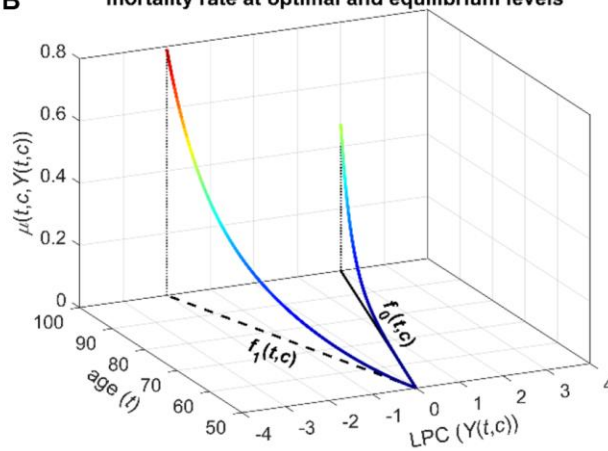


Supplementary Figure 8. Stochastic process models: Illustration of the mortality rate and the quadratic part in the hazard corresponding to different patterns of $f_0(t, c)$. (A) The quadratic part in the hazard in the case of the optimal trajectory increasing with age; (B) The quadratic part in the hazard corresponding to the optimal trajectory declining with age; (C) The mortality rate when the optimal trajectory increases with age; (D) The mortality rate when the optimal trajectory declines with age. For this illustration, we modeled Eqs. (6–7) with a single binary covariate c and parameters corresponding to a hypothetical biomarker $Y(t, c)$ (e.g., a transformed LPC) having the standard normal distribution and hazard rates resembling human mortality rates at old ages. Figure A, B show the quadratic parts in the hazard from Eq. (7) (i.e., $Q(t, c)(Y(t, c) - f_0(t, c))^2$) as a function of age t , covariate c (shown for $c = 0$), and the hypothetical biomarker $Y(t, c)$ for increasing (A) and declining (B) $f_0(t, c)$. The figures also display the optimal trajectories $f_0(t, c)$ (black lines) where the quadratic part equals zero so that the mortality rate is $\mu_0(t, c)$ (Eq. (7)). Respective mortality rates $\mu(t, c, Y(t, c))$ (Eq. (7)) are presented in (C, D). These figures also show the baseline mortality $\mu_0(t, c)$ (black lines) observed at the optimal levels $f_0(t, c)$. For simplicity of illustration, we assumed here that $Q(t, c)$ does not depend on age t so that the width of the U-shape of mortality as a function of the biomarker $Y(t, c)$ is the same for all ages.

A quadratic part in hazard at optimal and equilibrium levels

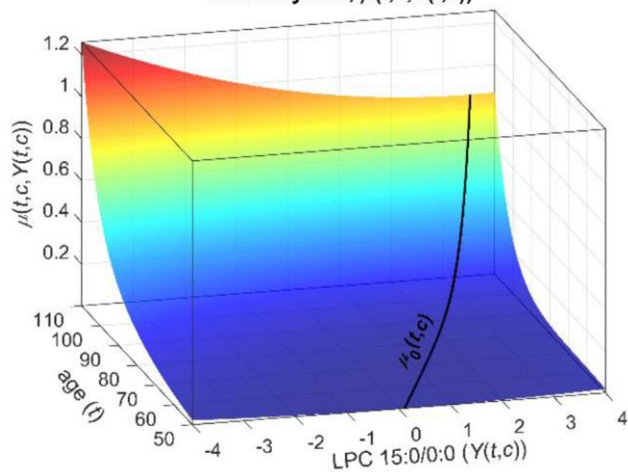


B mortality rate at optimal and equilibrium levels

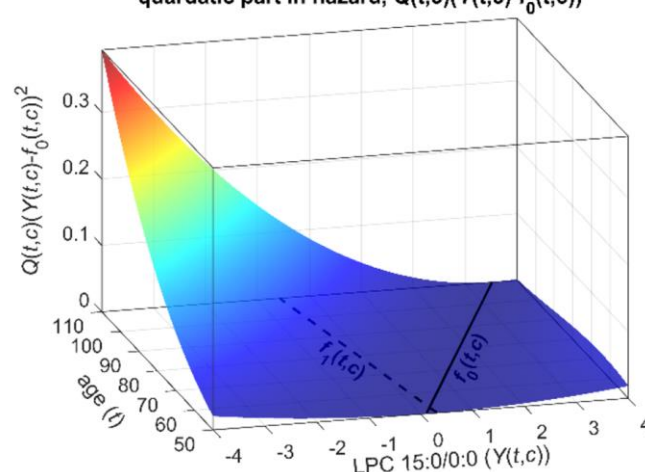


Supplementary Figure 9. Stochastic process models: Illustration of the quadratic part in the hazard and the mortality rate corresponding to equilibrium and optimal trajectories of the stochastic process $Y(t, c)$. The figure shows the quadratic part in the hazard $Q(t, c)(Y(t, c) - f_0(t, c))^2$ (A) and the mortality rate $\mu(t, c, Y(t, c))$ (B) from Eq. (7) for different values of age t , covariate $c = 0$, and the hypothetical biomarker $Y(t, c)$ evaluated at the optimal ($f_0(t, c)$, solid black lines) and equilibrium ($f_1(t, c)$, dashed black lines) levels for respective ages t and $c = 0$. For this illustration, we modeled Eqs. (6)-(7) with a single binary covariate c and parameters corresponding to a hypothetical biomarker $Y(t, c)$ (e.g., a transformed LPC) having the standard normal distribution and hazard rates resembling human mortality rates at old ages.

A mortality rate, $\mu(t, c, Y(t, c))$



B quadratic part in hazard, $Q(t, c)(Y(t, c) - f_0(t, c))^2$



Supplementary Figure 10: Stochastic process models: 3D plots illustrating results of applications to measurements of LPC 15:0/0:0 and mortality data in the LLFS. (A) Estimates of the mortality rate ($\mu(t, c, Y(t, c))$) as a function of age (t), covariates (c), and LPC 15:0/0:0 ($Y(t, c)$); (B) Estimates of the quadratic part in the equation for the hazard (mortality) rate ($\mu(t, c, Y(t, c)) - \mu_0(t, c)$) for different ages (t) and values of LPC 15:0/0:0 ($Y(t, c)$). The estimates are shown for zero (mean) values of binary (continuous) covariates c . The solid black lines denote the baseline mortality rate $\mu_0(t, c)$ (Supplementary Figure 10A) and the optimal trajectory $f_0(t, c)$ (Supplementary Figure 10B). The dashed black line corresponds to the equilibrium trajectory $f_1(t, c)$. LPC values were transformed (see Data).